REDUCING OBSERVATION TIME FOR RELIABLE CYCLOSTATIONARITY FEATURE EXTRACTION

Amy C. Malady (Wireless@VT, Virginia Tech, Blacksburg, VA, USA; amalady@vt.edu)
A. A. (Louis) Beex (Wireless@VT, Virginia Tech, Blacksburg, VA, USA; beex@vt.edu)

ABSTRACT

The reliability of second-order first-conjugate and sixth-order first-conjugate cyclostationarity feature extraction is improved for a subset of digital signals through the incorporation of robust statistics. The improvement is reflected in reduced minimum SNR and/or reduced minimum observation time for given performance. Two robust estimation methods – of different computational complexity – are contrasted. In most cases, a trade-off between SNR and computational complexity can be made and 1-2 dB of further improvement is realized by using the more complex influence function in the robust estimator. For the signals and observation times considered here, both robust methods yield reliability equivalent to that of the classic estimators of cyclostationarity at significantly reduced observation times.

1. INTRODUCTION

Cyclostationarity is a good feature for signal classification and detection as extracting cyclostationarity features can be done with minimal pre-processing tasks, i.e., bypassing tasks that require a priori knowledge of channel characteristics and signal parameters often unavailable during detection and classification stages [1]. Additionally, the incorporation of robust statistics successfully reduces SNR requirements for second-order cyclostationarity feature extraction [2] and improves QPSK symbol timing estimates when SNR is greater than or equal to 0 dB [3].

For some applications of interest, the most restrictive requirements for using cyclostationarity features is the long observation time required for reliable classification and detection. Previously published results using the second-order first-conjugate Cyclic Temporal Moment Function (CTMF) to classify a subset of analog and digital signals indicate an SNR requirement of 5 dB and an observation time of 6000 symbols to achieve reliable second-order first-conjugate cyclostationarity feature extraction [4].

In this work, we use a robust estimator of second-order first-conjugate cyclostationarity and provide a direct comparison of observation time requirements with a classic estimator. All else being equal, the robust estimator needs only 10% of the observation time of the classic estimator to achieve reliable feature extraction at 5 dB. Additionally, we extend the robust estimator to a higher-order feature which can be used to further distinguish QPSK signals from 8PSK signals. As a result of the incorporation of robust statistics, higher-order cyclostationarity feature extraction also experiences a reduction in required observation times for a given level of performance.

2. CYCLOSTATIONARITY DEFINITIONS

The *n*-th order *q*-conjugate lag product of $x(t)$, a generally complex signal normalized to have unit variance, is defined in (1) [7].

$$L_x(t,\boldsymbol{\tau})_{n,q} = \left(\prod_{j=1}^{n} x^{(*)}(t+\tau_j)\right); \boldsymbol{\tau} = \begin{bmatrix}\tau_1 & \cdots & \tau_n\end{bmatrix} \qquad (1)$$

The symbol (*) denotes optional conjugation, such that there are *q* conjugations in total, and $\boldsymbol{\tau}$ is the delay vector. For all results reported here, $\boldsymbol{\tau} = \mathbf{0}$. A signal exhibits *n*-th order *q*-conjugate cyclostationarity if there exists an $(\alpha, \boldsymbol{\tau})$ pair, for $\alpha \neq 0$, for which the lag product contains discrete spectral components [2]. Any such α is called a cycle frequency (CF). Given a finite observation of the signal $x(t)$, the classic estimate of the spectral content of the lag product, the Cyclic Temporal Moment Function Estimate (CTMFE), can be found as in (2) [7].

$$\hat{R}_x^{\alpha}(\mathbf{0})_{n,q} = \frac{1}{T}\sum_{t=0}^{T} L_x(t,\mathbf{0})_{n,q} e^{j2\pi\alpha t} \qquad (2)$$

While the ideal CTMF will be nonzero only at cycle frequencies, finite estimation errors will cause the CTMFE to contain nonzero spectral content at non-cycle frequencies. Additionally, in wireless communications, the available signal is often contaminated by environmental factors, e.g., additive noise, such that the lag product is no longer a function of only the desired signal $s(t)$. In the AWGN model, the desired signal is contaminated by complex Gaussian noise $n(t)$, producing the received signal $r(t)$.

$$r(t) = s(t) + n(t) \tag{3}$$

Robust techniques have been proposed to mitigate the influence of outliers in $r(t)$ when trying to estimate the underlying statistics of the desired signal $s(t)$ [5]. As was demonstrated in previous work [3], robust techniques mitigate the SNR requirements on $r(t)$ when estimating cyclic statistics, specifically the CTMFE, when SNR requirements are at or above 0 dB. In this work, we explore how robust techniques can reduce observation time requirements as well as SNR requirements.

To find the robust CTMFE, the data is first normalized by the robust estimate of scale, the Complex Median Absolute Deviation (CMAD) from the mean, rather than the traditional variance. The (CMAD) of an arbitrary complex signal $x(t)$ is defined in (4).

$$CMAD \triangleq 1.2011 med\,|\,x(t)\,| \tag{4}$$

An influence function $\Psi(x)$ can be used to modify the data such that samples are preferentially weighted based on their magnitude [3]. While many influence functions have been defined, we limit our present consideration to the two influence functions, $\Psi_1(x)$ and $\Psi_2(x)$, defined below.

$$\Psi_1(x) = \begin{cases} x & for\,|x| \le a \\ a\dfrac{x}{|x|} & for\,|x| > a \end{cases} \tag{5}$$

$$\Psi_2(x) = \begin{cases} x & for\,|x| \le a \\ 0 & for\,|x| > a \end{cases} \tag{6}$$

The influence function described by (5) is commonly referred to as Huber's function, and is widely accepted as an ideal choice for many applications. Note that the phase information of a complex signal is preserved by Huber's function. The influence function in (6), on the other hand, can be computationally more efficient.

The choice of *a* impacts the percentage of the data that will be modified according to (5) and (6). The value of *a* was determined heuristically, and is so far unique to the choice of influence function. The choice of *a* will be specified in the results section.

Using an influence function, the choice of which is indicated by index *m*, the robust *n*-th order *q*-conjugate lag product is given in (7).

$$L_{\Psi_m(x)}(t,\boldsymbol{\tau})_{n,q} = \left(\prod_{j=1}^{n} \Psi_m^{(*)}\left(\frac{x(t+\tau_j)}{CMAD} \right) \right); \boldsymbol{\tau} = [\tau_1 \quad \cdots \quad \tau_n] \tag{7}$$

Finally, the robust CTMFE is found from the robust lag product as given in (8).

$$\tilde{R}_x^{\alpha}(\mathbf{0})_{n,q} = \frac{CMAD^n}{Tc} \sum_{t=0}^{T} L_{\Psi_m(x)}(t,\mathbf{0})_{n,q} e^{j2\pi\alpha t} \tag{8}$$

The term $CMAD^n (Tc)^{-1}$ is included for scaling and Fisher consistency, but given the nature of our classifier, it is not necessary, as will be shown in the next section.

The digital signals of interest contain second-order first-conjugate cyclostationarity and therefore have a cycle frequency, which corresponds to the symbol rate, in the second-order first-conjugate CTMF. Figure 1 shows the classic and robust estimates, respectively, of the second-order first-conjugate CTMFE of a QPSK signal in 2 dB SNR with an observation time of 3000 symbols. The robust estimate is found using Huber's function with $a = 1$.

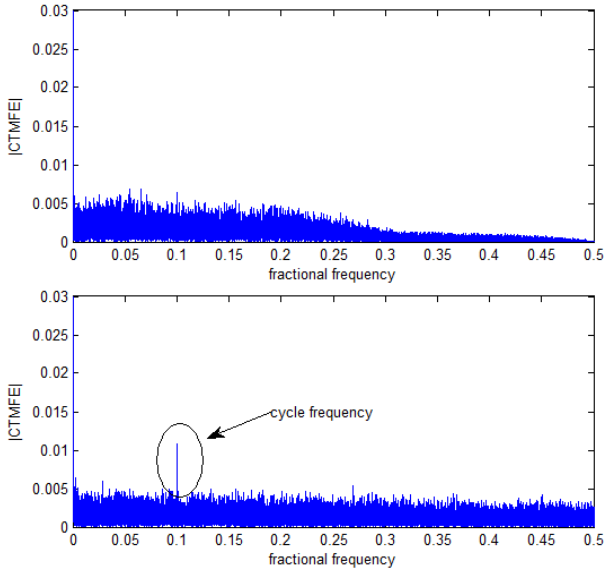

Figure 1 The classic (top) and robust (bottom) second-order first-conjugate CTMFE based on a QPSK signal in additive noise at 2 dB SNR and an observation window of 3000 symbols.

Observe that in the robust estimate the peak at the cycle frequency is prominent while in the classic estimate it is not.

The prominence of the CTMFE at a cycle frequency in the robust estimate motivates the investigation of robust estimators to improve the reliability and practicality of using cyclostationarity features for detection and classification.

3. STATISTICAL TEST FOR CYCLOSTATIONARITY

Both the robust and classic CTMFE have spectral content at non-cycle frequencies, as seen in Fig. 1. At low enough SNR and short enough observation times, it is possible that the peaks at a non-CF appear as distinct as those at CFs. A statistical test was proposed in previous work as a solution

to determining the statistical significance of peaks in the CTMFE [6]. In summary, the statistic test is applied at each candidate cycle frequency $\hat{\alpha}$ according to the procedure below. The outcome of the test is a test statistic which can be compared against a threshold for statistical significance. Justification for the test is provided elsewhere [6].

The test procedure for CF presence, using the classic CTMFE, is as follows. Estimate $\hat{R}_x^{\hat{\alpha}}(\mathbf{0})_{n,q}$, according to (2), where $\hat{\alpha}$ is a candidate CF. From $\hat{R}_x^{\hat{\alpha}}(\mathbf{0})_{n,q}$, create the row vector $\hat{\mathbf{c}}$.

$$\hat{\mathbf{c}} = [\mathrm{Re}(\hat{R}_x^{\hat{\alpha}}(\mathbf{0})_{n,q}) \quad \mathrm{Im}(\hat{R}_x^{\hat{\alpha}}(\mathbf{0})_{n,q})] \tag{9}$$

Next, estimate the unconjugated $\hat{S}_{n,q}^{(T)}$ and conjugated $\hat{S}_{n,q}^{(T^*)}$ cyclic spectrum.

$$\hat{S}_{n,q}^{(T)} = \frac{1}{TL}\sum_{s=-\frac{(L-1)}{2}}^{s=-\frac{(L-1)}{2}} W(s)\hat{R}_x^{\hat{\alpha}-\frac{2\pi s}{T}}(\mathbf{0})_{n,q}\hat{R}_x^{\hat{\alpha}+\frac{2\pi s}{T}}(\mathbf{0})_{n,q} \tag{10}$$

$$\hat{S}_{n,q}^{(T^*)} = \frac{1}{TL}\sum_{s=-\frac{(L-1)}{2}}^{s=-\frac{(L-1)}{2}} W(s)\hat{R}_x^{\hat{\alpha}+\frac{2\pi s}{T}}(\mathbf{0})_{n,q}\left(\hat{R}_x^{\hat{\alpha}+\frac{2\pi s}{T}}(\mathbf{0})_{n,q}\right)^* \tag{11}$$

where $W(s)$ is a window of length L, used for smoothing in the "spectral" domain. A 61-point Kaiser window is used.

Using (10) and (11) assemble the covariance matrix estimate $\hat{\Xi}_{n,q}$.

$$\hat{\Xi}_{n,q} = 0.5\begin{bmatrix} \mathrm{Re}\left(\hat{S}_{n,q}^{(T)} + \hat{S}_{n,q}^{(T^*)}\right) & \mathrm{Im}\left(\hat{S}_{n,q}^{(T)} - \hat{S}_{n,q}^{(T^*)}\right) \\ \mathrm{Im}\left(\hat{S}_{n,q}^{(T)} + S_{n,q}^{(T^*)}\right) & \mathrm{Re}\left(\hat{S}_{n,q}^{(T^*)} - \hat{S}_{n,q}^{(T)}\right) \end{bmatrix} \tag{12}$$

The test statistic $\Upsilon_{n,q}$ is then found as follows.

$$\Upsilon_{n,q} = T\hat{\mathbf{c}}\hat{\Xi}_{n,q}^{-1}\hat{\mathbf{c}}^T \tag{13}$$

The distribution of the test statistic at a non-CF follows a chi-squared distribution with two degrees of freedom regardless of the distribution of the underlying data set [6].

Recall that the robust CTMFE in (8) is normalized by $\chi = CMAD^n(Tc)^{-1}$. Of particular interest here is to demonstrate that the normalization constant does not influence the distribution of the test statistic at non-CFs. Consider the following reorganization of $\tilde{R}_x^{\hat{\alpha}}(\mathbf{0})_{n,q}$.

$$\begin{aligned} \tilde{F}_x^{\hat{\alpha}}(\mathbf{0})_{n,q} &= \sum_{t=0}^{T} L_{\Psi(x)}(t,\mathbf{0})_{n,q} e^{j2\pi\hat{\alpha}t} \\ \tilde{R}_x^{\hat{\alpha}}(\mathbf{0})_{n,q} &= \chi\tilde{F}_x^{\hat{\alpha}}(\mathbf{0})_{n,q} \end{aligned} \tag{14}$$

The robust cumulant estimate $\tilde{\mathbf{c}}$ is expressed as follows

$$\begin{aligned} \tilde{\mathbf{c}} &= \chi[\mathrm{Re}(\tilde{F}_x^{\hat{\alpha}}(\mathbf{0})_{n,q}) \quad \mathrm{Im}(\tilde{F}_x^{\hat{\alpha}}(\mathbf{0})_{n,q})] \\ &= \chi\tilde{\mathbf{d}} \end{aligned} \tag{15}$$

The robust estimates of the conjugated $\tilde{S}_{n,q}^{(T^*)}$ and unconjugated $\tilde{S}_{n,q}^{(T)}$ cyclic spectrum are given below,

$$\begin{aligned} \tilde{S}_{n,q}^{(T^*)} &= \frac{1}{TL}(\chi)^2 \sum_{s=-\frac{(L-1)}{2}}^{s=-\frac{(L-1)}{2}} W(s)\tilde{F}_x^{\hat{\alpha}+\frac{2\pi s}{T}}(\mathbf{0})_{n,q}\left(\tilde{F}_x^{\hat{\alpha}+\frac{2\pi s}{T}}(\mathbf{0})_{n,q}\right)^* \\ &= (\chi)^2\tilde{P}_{n,q}^{(T^*)} \end{aligned} \tag{16}$$

$$\begin{aligned} \tilde{S}_{n,q}^{(T)} &= \frac{1}{TL}(\chi)^2 \sum_{s=-\frac{(L-1)}{2}}^{s=-\frac{(L-1)}{2}} W(s)\tilde{F}_x^{\hat{\alpha}-\frac{2\pi s}{T}}(\mathbf{0})_{n,q}\tilde{F}_x^{\hat{\alpha}+\frac{2\pi s}{T}}(\mathbf{0})_{n,q} \\ &= (\chi)^2\tilde{P}_{n,q}^{(T)} \end{aligned} \tag{17}$$

and the robust covariance estimator $\tilde{\Xi}_{n,q}$ in (18) follows.

$$\begin{aligned} \tilde{\Xi}_{n,q} &= 0.5(\chi)^2\begin{bmatrix} \mathrm{Re}\left(\tilde{P}_{n,q}^{(T)} + \tilde{P}_{n,q}^{(T^*)}\right) & \mathrm{Im}\left(\tilde{P}_{n,q}^{(T)} - \tilde{P}_{n,q}^{(T^*)}\right) \\ \mathrm{Im}\left(\tilde{P}_{n,q}^{(T)} + \tilde{P}_{n,q}^{(T^*)}\right) & \mathrm{Re}\left(\tilde{P}_{n,q}^{(T^*)} - \tilde{P}_{n,q}^{(T)}\right) \end{bmatrix} \\ &= (\chi)^2\tilde{\Theta}_{n,q} \end{aligned} \tag{18}$$

Finally, the robust test statistic $\tilde{\Upsilon}_{n,q}$ in (19) results.

$$\tilde{\Upsilon}_{n,q} = T\chi\tilde{\mathbf{d}}\left(\chi^2\tilde{\Theta}_{n,q}\right)^{-1}\chi\tilde{\mathbf{d}}^T \tag{19}$$

Using basic rules of algebra and the property that $[kA]^{-1} = k^{-1}A^{-1}$, where k is a constant and A is a square matrix, the final robust test statistic is seen to be independent of the scaling constant $\chi = CMAD^n(Tc)^{-1}$, and given by the reduced expression in (20).

$$\tilde{\Upsilon}_{n,q} = T\tilde{\mathbf{d}}\tilde{\Theta}_{n,q}^{-1}\tilde{\mathbf{d}}^{T} \quad (20)$$

Since the scaling constant does not appear in the final test statistic in (20), the only impact of applying the Huber function is a change in the distribution of the data set, but this change does not introduce cyclostationarity. Therefore, at non-CFs the robust test statistic also follows a chi-squared distribution with two degrees of freedom [3]. The knowledge of the distribution of the test statistic at non-CFs can be used to set tolerable false alarm thresholds for either method – classical or robust – of estimating the CTMF.

4. SIGNALS OF INTEREST

Second-order first-conjugate and sixth-order first-conjugate cyclostationary features can be used to distinguish a subset of analog and digital signals. Particularly, the absence or presence of second-order first-conjugate cyclostationarity can be used to distinguish SSB and DSB signals from MPSK signals, as was done in previous work [4]. The analog signals, in particular, do not exhibit second-order first-conjugate cyclostationarity, while the digital signals do.

Further, sixth-order first-conjugate cyclostationarity can be used to distinguish QPSK signals from 8PSK signals, as indicated in previous work [7]. Since we have shown that the behavior of the test statistic at non-CFs is unaffected by the incorporation of robust statistics, we will not study the entire classification problem here, but rather focus on how robust statistics improve the reliability of extracting cyclostationarity features. The classification problem is only one example of when cyclostationarity features are useful.

Feature extraction will be done at baseband, such that the (baseband) signals $r(t)$ at the input of a receiving filter are of the form,

$$r(t) = \exp\left(j\left(2\pi\Delta f_c t + \varphi\right)\right)s(t) + n(t) \quad (21)$$

where Δf_c is the carrier frequency offset and φ is the random phase offset. The signal of interest is $s(t)$ and $n(t)$ is uncorrelated complex zero mean Gaussian noise. The entire received signal is then filtered such that the noise is no longer white.

The digital signals of interest in this work are BPSK, QPSK, and 8PSK signals. The signals are RC-pulse shaped with a pulse shape parameter of 0.25. The symbol rate is 10,000 symbols per second, and the signal is oversampled by a factor of 10 such that the sampling rate is F_s = 100 kHz. The noise bandwidth of the receiver is $0.25F_s$, the phase offset is a uniform random variable, and the carrier frequency offset is $\Delta f_c = 0.01F_s$.

All of these digital signals have a second-order first-conjugate CF corresponding to their symbol rate [4]. Additionally, BPSK and QPSK signals both have a sixth-order first-conjugate CF corresponding to $4\Delta f_c$ [7].

5. SIMULATION RESULTS

First, we compare the behavior of the classic and robust test statistic when calculated at the known second-order first-conjugate cycle frequency of 10 kHz. The threshold for statistical significance was set at 13.814, which corresponds to a false alarm rate of 0.1% [8].

In each trial, a long version of each signal: BPSK, QPSK, and 8PSK - is generated and then segmented based on the observation time of interest. Based on the same observation data, two robust test statistics and a classic test statistic are calculated. The robust test statistics are calculated using the influence functions in (5) and (6).

The resulting test statistics are compared to the threshold for statistical significance. If the test statistic exceeds the threshold, the test successfully detected the second-order first-conjugate cyclostationarity; otherwise the test failed to detect the cyclostationarity. The detector is not given any information about SNR or the phase offset, but is provided with the location of the cycle frequency.

A choice of a = 1 in the Huber influence function (5) is used based on recommendations in the literature [3]. A choice of a = 1.2011 is used for the second influence function $\Psi_2(x)$. This choice of a reflects the best choice for maximizing detection rates based on preliminary experimental results which considered a range of $1 \le a \le 2$. This specific value of a was investigated because it appears as the normalization constant in (4); however, it is not guaranteed to be the optimal choice.

Figure 2 illustrates the probability of detecting the cyclostationarity feature in each of the digital signals when the observation window is 1500 symbols.

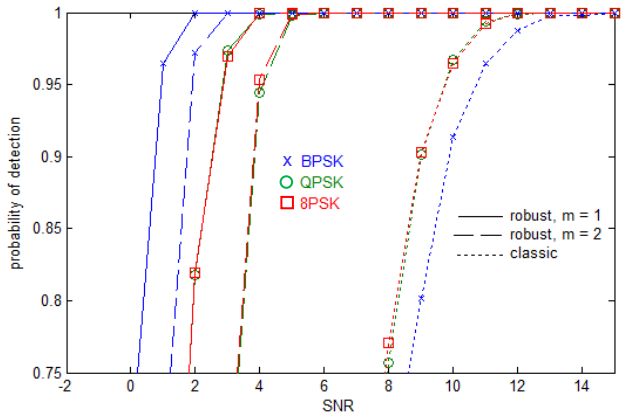

Figure 2 Detection curves for the robust (using $\Psi_1(x)$ and $\Psi_2(x)$) and classic statistical tests of second-order first-conjugate cyclostationarity. The observation time is 1500 symbols and the threshold for statistical significance is 13.814.

Observe that the robust detector using $\Psi_1(x)$ achieves reliable detection in all three cases at 4 dB SNR. The robust detector using $\Psi_2(x)$ achieves reliable detection in all three cases at 5 dB SNR. However, the classic detector has a much higher SNR requirement of at least 13 dB.

Note also in Fig. 2 that the robust detection curves are much steeper than the classic detection curves, which indicates that an increase in SNR yields better performance more quickly when using the robust estimator than when using the classic estimator of the CTMF.

The reduced SNR requirements enjoyed by the robust estimators, as compared to the classic estimator, vary as a function of observation time. Figure 3 illustrates the relationship between observation time and minimum SNR required for reliable detection; the notation (x;y)% reliability is used to indicate >x% probability of detection at <y% false alarm probability. The classic detector has significantly worse detection rates than either of the robust detectors; therefore it was not possible to plot the minimum SNR requirements for short observation times since they exceeded the maximum simulated SNR of 15 dB.

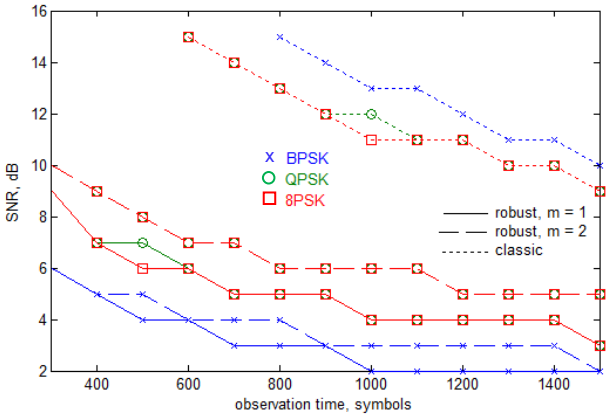

Figure 3 Minimum SNR requirements as a function of observation time for reliable detection of second-order first-conjugate cyclostationarity. The robust (solid) curves represent (99;0.1)% reliability while the classic (dashed) curves represent (90;0.1)% reliability.

In Fig. 3, the reliability of the classic detector is only at least 90% for the indicated SNR and observation time, whereas the robust detectors have a detection reliability of at least 99% for all plotted SNR and observation times.

The robust test statistic associated with using the influence function $\Psi_1(x)$ for all three digital signals of interest is statistically significant in 99% of the trials for an observation time of 400 symbols and an SNR of at least 7 dB. The robust test statistic associated with using the influence function $\Psi_2(x)$ for all three digital signals of interest is statistically significant in 99% of the trials for an observation time of 400 symbols and an SNR of at least 9 dB. The classic test statistic is not statistically significant for even 90% of the time when given an observation time almost 4 times as long – 1500 symbols – and an SNR of 9 dB.

As observed in Fig. 3, for the studied observation times, the reduction in SNR requirements when using influence function $\Psi_1(x)$ is at least 5 dB for all signals. Moreover, at 10 dB, the robust estimator needs less than 20% of the observation time required by the classic estimator while providing better detection. In exchange for using the less computationally complex influence function $\Psi_2(x)$, the SNR requirements are reduced by at least 4 dB. In general, the more complex influence function yields an additional 1 dB improvement in comparison to the less complex influence function.

Previously published results report that a 6000 symbol observation time and an SNR of 5 dB is needed to achieve reliable detection of cyclostationarity when using classic estimation techniques [2]. The robust estimator using $\Psi_1(x)$ achieves reliable detection for an observation time of 600 symbols at SNR of about 5 dB. Therefore, there exist some cases where the robust estimator, all else being equal, only needs 10% of the data required by the classic estimator of cyclostationarity. This reduction in observation time requirements improves the practicality of using cyclostationarity feature-based detectors and classifiers.

While not explored in depth here, the results in Figs. 2 and 3 along with the visual improvements in the CTMFE seen by using the robust estimator in Fig. 1 suggest that the use of robust estimators would improve the performance of a blind statistical test, where the CF is unknown and a search over the CTMFE is necessary to determine candidate cycle frequencies. Previous results [2] already have shown that for long observation times blind classification is possible, and it is likely that reliable blind classification can be done for shorter observation times as well by using robust estimators of cyclostationarity.

In a similar fashion to the second-order first-conjugate cyclostationarity detection trials, trials were conducted to compare the statistical significance of the sixth-order first-conjugate classic and robust test statistic at known cycle frequencies. In these trials, only BPSK and QPSK signals are considered, as 8PSK signals do not contain discrete spectral content in their CTMF. The robust test statistics and classic test statistics are again computed based on the same data set. The same threshold of 13.814 is used to determine statistical significance. A choice of c = 1.8 was used for the influence function $\Psi_2(x)$ as this consistently yielded the best detection rate in preliminary trials.

The probability of detection versus SNR curves are shown in Fig. 4. The observation time is 1000 symbols. In both the robust and classic case, there is considerable difference in SNR requirements for BPSK and QPSK signals. When using influence function $\Psi_2(x)$ the use of robust estimation techniques alleviates SNR requirements by only 1-2 dB.

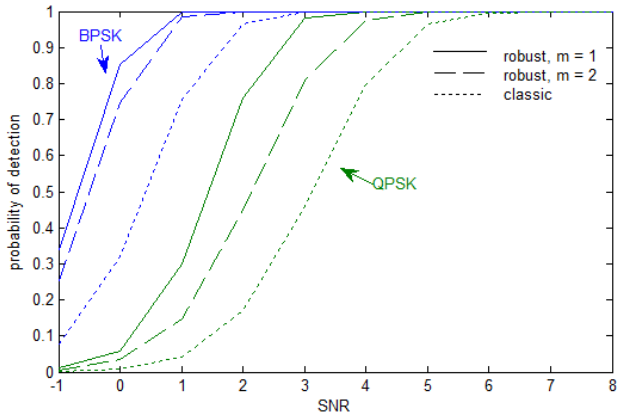

Figure 4 Detection curves for the robust and classic statistical tests of sixth-order first-conjugate cyclostationarity. Observation time 1000 symbols; threshold for statistical significance is 13.814.

Using the more complex influence function $\Psi_1(x)$, it is possible to achieve 2-3 dB improvements when estimating the cyclostationarity features of QPSK signals. Interestingly, there is little additional performance gain for BPSK signals.

The SNR improvements, in the sixth-order first-conjugate case are less dependent on the observation window – compare Figs. 3 and 5 – than in the second-order first-conjugate case.

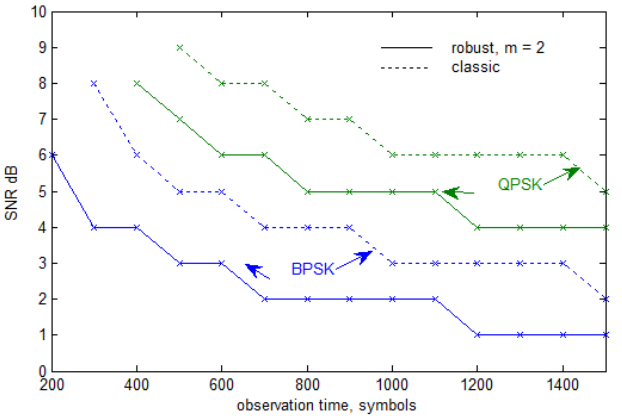

Figure 5 Minimum SNR requirements as a function of observation time for (99;0.1)% reliable detection of second-order first-conjugate cyclostationarity.

The robust estimator consistently enjoys a 1-2 dB improvement across observation window size. Unlike before, the plotted curves indicate the minimum requirements for (99;0.1)% reliability in both cases. In Fig. 5 only the results for the less complex influence function $\Psi_2(x)$ are plotted. In the case of BPSK, the two reliability lines associated with $\Psi_m(x)$, for m = 1 and m = 2, are equivalent. For all QPSK cases, the more complex influence function provides an additional improvement of 1 dB.

While the improvements at the higher-order cyclostationarity feature are not as profound, it is encouraging that robust techniques continue to provide improvement.

Since this was, to the best of our knowledge, the first investigation into robust techniques for higher-order cyclostationarity, it is possible that a better choice of a or a better choice of the influence function could provide more performance enhancement. Further investigation is needed to understand how well the robust estimator improves overall classifier performance at shorter observation times with the additional challenge of unknown CF location(s).

6. CONCLUSION

We have presented a novel application of robust estimators to mitigate the long observation time requirements of cyclostationarity feature extraction.

All else being equal, for an observation time of 1500 symbols, the robust estimator of second-order first-conjugate cyclostationarity has an SNR requirement which is at least 7 dB less than for the classic estimator. Additionally, the robust estimator of second-order first-conjugate cyclostationarity enjoys (99;0.1)% reliable classification at an SNR of about 5 dB and an observation time of 600 symbols, while the classic estimator needs an observation time of 6000 symbols to achieve (99;1)% reliable classification at 5 dB. For this case, the robust estimator alleviates the observation time requirements by a practically significant 90%.

While not as dramatic, using the robust estimator of sixth-order first-conjugate cyclostationarity in BPSK and QPSK signals consistently reduced SNR requirements by 1-2 dB or observation time requirements by 35 to 50%.

7. REFERENCES

[1] W. Gardner, A. Napolitano, and L. Paura, Cyclostationarity: half a century of research, Signal Processing 86 (4), pp. 639–697, 2006.

[2] A. C. Malady and A. A. (Louis) Beex, "AMC Improvements from Robust Estimation", Proc. GLOBECOM, pp. 1-5, 2010.

[3] T. Biedka, L. Mili, and J. H. Reed, "Robust estimation of cyclic correlation in contaminated Gaussian noise", *Proc. 29th Asilomar Conference on Signals, Systems and Computers*, pp. 511-515, Pacific Grove, CA, 1995.

[4] O. A. Dobre, A. Abdi, Y. Bar-Ness, and W. Su, "Cyclostationarity based blind classification of analog and digital modulations," *Proc. IEEE MILCOM*, Washington DC, USA, 2006.

[5] P. J. Huber, Robust Statistics, Wiley, 1981.

[6] A. V. Dandawade and G. B. Giannakis, "Statistical tests for presence of cyclostationarity," *IEEE Trans*. SP, vol. 42, pp. 2355- 2369, 1994.

[7] W. A. Gardner, Cyclostationarity in Communications and Signal Processing. New York: IEEE Press, 1993.

[8] A. Leon-Garcia, Probability and Random Processes for Electrical Engineering, Don Mills, Ont., Canada: Addison-Wesley, 1989.